Elastic constants and homogenized moduli of manganese carbonate structure based on molecular dynamics and Reuss-Voigt-Hill methods

Jia Fu[1,2 a], Hao Bai[1], Zhaoyuan Zhang[3] and Weihui Lin[4]

[1]School of Materials Science and Engineering, Xi'an Shiyou University, Xi'an, 710065, China

[2]LGCGM, National Institute of Applied Sciences, INSA-Rennes, Rennes, 35708, France

[3]School of Mechanical Engineering, Xi'an Shiyou University, Xi'an, 710065, China

[4]College of Mechanics, Taiyuan University of Technology, Taiyuan 030024, China

*Corresponding author: [a] fujia@xsyu.edu.cn

Abstract. With the development of computer technology, the crystal structure of atomic-scale dynamics simulation is a hot research in recent years. The manganese carbonate crystal structure is chosen as the research object, as the elasticity of manganese carbonate crystal structure has been studied based on the plane wave ultra-soft first-principles density functional theory framework pseudopotential method. Based on molecular dynamics , interatomic potential function was introduced to describe the interactions between atoms of manganese carbonate crystals and then elasticity contants of manganese carbonate crystals, bulk modulus, shear modulus, Young's modulus were simulated. Influencing of the pressure on elastic properties has been studied, the results indicate that: 1) the structure of manganese carbonate crystal shows anisotropy due to the different types of atoms of Coulomb force and van der Waals forces; 2) elastic moduli are also obtained, of which the bulk modulus B is 107.682GPa, shear modulus G is 52.09GPa; 3) the values are very consistent to the results of Chen (B 108GPa and G 49.8GPa), thus the established model and the selected potential functions are verified to be reliable.

1. Introduction

Elastic properties of crystals involves a number of fields, including chemical composition, crystal orientation, pressure and temperature. The molecular dynamics (MD) and Monte Carlo (MC) are mainly used to study molecular structure and dynamics[1]. Chen et al. [2] have studied elastic modulus of manganese carbonate single crystal measured by Brillouin spectroscopy, and the elastic constants (C_{11}, C_{12}, C_{13}, C_{14}, C_{33} and C_{44}) of the triangular crystal structure at constant temperature are as: 223.9 GPa, 93.4 GPa, 76.0 GPa, -17.3 GPa, respectively. 132.6 GPa and 44.5 GPa, which are in good aggrement with the ultrasound experiment data, with rigid modulus value of 108 GPa. Wang et al. [3] have calculated the bulk modulus of manganese carbonate crystal, with its value 135GPa based on MD theory. Zhang et al. [4] have done the X-ray energy diffraction experiment of manganese carbonate crystal and obtained the rigid modulus 108 GPa by means of energy dispersion analysis. At present, researches on the structure of carbonic acid crystal mainly includes: the evaluation of lattice

parameters, structural characteristics, the measurement of bulk modulus, and the prediction of elastic constants [3, 5].

However, its systematically parameters of manganese carbonate crystal have not been studied yet. This work focus on the effect of pressure on the elastic properties of manganese carbonate crystal structures under certain temperature conditions. The obtained elastic constants are as: C_{11} is 197.89 GPa, C_{12} 61.19 GPa, C_{13} 62.88 GPa, C_{14} 14.13 GPa, C_{33} 198.97 GPa, C_{44} 37.84 GPa. Besides, the bulk modulus and shear modulus are separately 107.63 GPa and 52.09 GPa, which is closer to the experimental values of bulk modulus 114.3 GPa and shear modulus 49.8 GPa in literature [2]. Elastic moduli of various typical crystals can be calculated by the calssical Reuss-Voigt-Hill method [6-10]. These conclusions are useful for the molecular dynamics study of similar crystal structure with the space group $R\bar{3}C$ at nanoscale.

2. Modelling and potential functions

2.1 Modelling of manganese carbonate crystal

Manganese carbonate crystals belong to the trigonal system, the space group is $R\bar{3}C$ type, and the lattice parameters are: a=b=4.772Å, c=15.637Å, α=90°, β=90°, γ=120°. Its crystal structure is shown in Fig.1.

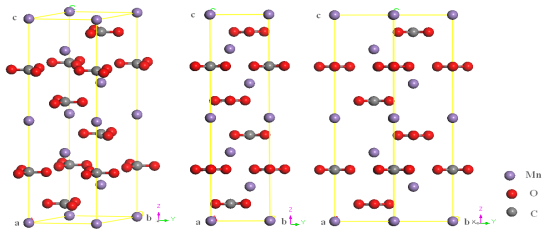

(a) atomic structure

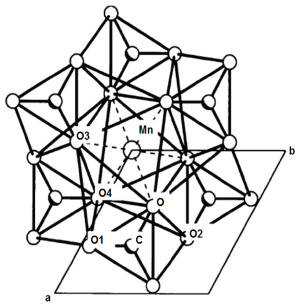

(b) CO_3 group

Figure 1. Schematic diagram of manganese carbonate crystal structure.

As in Fig.1(a), the crystal has characteristics as follows: 1) two Mn atoms are attached to anion groups (CO_3^{-2}), forming into an equilateral triangle; 2) the triangle consists of a central carbon atom and a total of 3 oxygen atoms per vertex.

From Fig.1 (b), the atomic spacing of the CO3 groups is as: C-O bond is 1.2867 Å, Mn-O^{i} is 2.1920 Å, O-O^{i} is 2.9544 Å, O-O^{ii} is 2.2282 Å, O-O^{iii} is 3.0531 Å, O-O^{iv} is 3.1467 Å. Moreover, it can be seen that the CO_3 group also has an interaction potential with the peripheral oxygen atoms in addition to the Morse potential between C-O in the CO_3 group. That is to say, there are van der Waals force and Coulomb force between O-O and Mn-O.

In order to maintain the 120° invariance of the CO_3 group, the tri-atomic potential function of the O-C-O and the tetra-atomic potential function of O-C-O-O outside the C plane in the CO_3 group structure are introduced into the manganese carbonate model.

2.2 Interaction potential functions

2.2.1 Parameters of potential functions

The charge distribution of each ion of manganese carbonate crystal is as follows: Mn is +2.633 C, C is +1.646 C, each O is -1.426 C, single O_c (core) is +0.4345 C, single O_s(shell) is -1.4345 C. Then the corresponding Buckingham potential can be calculated. The potential function parameter is in Table 1.

Table 1. Parameters of potential functions between atoms.

(a) Morse potential

	C_c - O_c[3]
De(eV)	4.71
a($Å^{-1}$)	3.8
r_0(Å)	1.18

(b) Buckingham potential

	O_c - O_c	O_s - O_s	Mn_c-O_s[5]	Mn_c-C_s[5]	O_c-Mn_c[3]
A(eV)	4030.3	214836.2	1039.59	98181818.2	6348.6
ρ(Å)	0.217	0.198	0.289	0.120	0.2293
C($eVÅ^6$)	0	21.61	0	0	0

(c) Multi-body potentials

The three-body potentials		The four-body potentials	
O-C-O		O-C-O-O	
k_2 (eV/rad^2)	1.799	k(eV)	8.689
θ_0(°)	120	φ(°)	360°

(d) Harmonic spring potential

	O_c – O_s
k_2 ($eV·Å^{-2}$)	52.740

For atomic potentials, the potential functions of Mn-C and Mn-Os can be used by the data of the literature [11], and the appropriate parameters (De, a, $_0$ et k_2) of the others potential functions are selected according to different atomic types.

2.2.2 Interaction potential curves

The interaction potential curve between different atoms in manganese carbonate crystal is shown in Fig. 2.

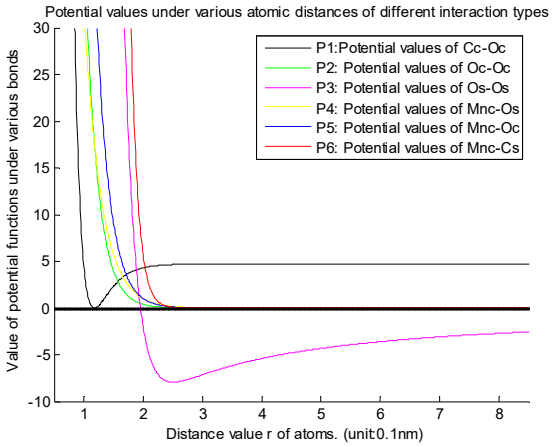

Figure 2. Curves of interaction potential between various atoms of crystal.

Based on potential functions in Figure 2, the atomic position and lattice parameters are optimized during the energy minimization at a constant pressure[6-7]. The Newtonian iterative method is used to search for the minimum value in simulation process.

3. Result analysis and discussion

3.1 Lattice parameters and elastic constants

3.1.1 Lattice parameters

The lattice parameter *a*(Å), *b*(Å), *c*(Å), volume(Å^3) at 0MPa are shown in Table 2.

Table 2. Lattice *a*, *b*, *c* (Å) of manganese carbonate crystal.

	a,b	c	V
Present	4.7574	15.7542	308.77
Exp.[12]	4.772	15.637	308.38
Exp.[3]	4.55	15.91	285.24

The c/a ratio used is 3.285, within the relative error range of the experiment, which match better to Maslen [12] 3.276, Wang [3] 3.49 and Zhang [4] 3.31. Besides, the variation slopes of *a* and *c* are -0.0506 and -0.0153, which is close to the slopes of *a* and *c* values -0.0640 and -0.0120 by Zhang[4].

3.1.2 Elastic constants

Elastic constants C_{ij} (GPa) of manganese carbonate crystal is shown in Table 3.

Table 3. Elastic constants C_{ij} of manganese carbonate crystal.

	C_{11}	C_{12}	C_{13}	C_{14}	C_{33}	C_{44}
Present	197.89	61.19	62.88	14.13	198.97	37.84
Exp.[2]	223.9	93.4	76.0	-17.3	132.6	44.5

From Table 3, it can be seen that C_{33} is the largest, indicating that the stiffness in this direction is the largest. Elastic constants C_{ij} under various pressures within the rangge of 0-350GPa is in Fig.3.

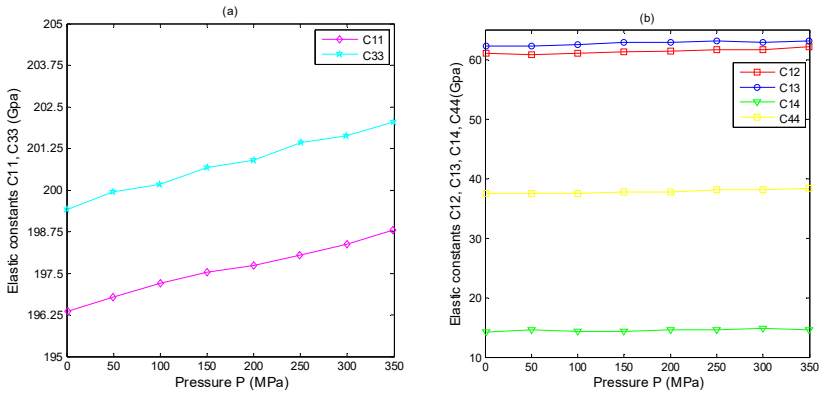

Figure 3. Elastic constants C_{ij} under different pressures.

From Fig. 3(a), the variation of elastic constants under different pressures is not the same, where the slope of the C_{11} and C_{33} change curves is positive. C_{33} in *c*-axis direction is perpendicular to the atomic plane composed of *a*-axis and *b*-axis. The contribution of C_{33} to elasticity is greater than that of the *a*-axis C_{11} and the *b*-axis C_{22}. The rest elastic constants slightly increased but tended to be relatively steady.

3.2 Reuss bound and Voigt bound

3.2.1 The compliance coefficient S_{ij}

For trigonal crystals, the elastic constants need to satisfy the generalized stability criteria [13]: $C_{11}>|C_{12}|$, $(C_{11}+C_{12})C_{33}-2C_{13}^2>0$, $(C_{11}-C_{12})C_{44}-2C_{14}^2>0$; Elastic constant characterizes the response of the lattice to external stress within the elastic limit [8]. Young's modulus describes the linear deformation behaviors of the crystal, its value in three directions of *a*, *b*, and *c* axes can be obtained from the inverse S_{ij} matrix in Cartesian coordinates: $E_x = S_{11}^{-1}$, $E_y = S_{22}^{-1}$, And $E_z = S_{33}^{-1}$. The compliance coefficient S_{ij} can be obtained by inverse matrix of the expression ($S = C^{-1}$).

$$S_{11}=\frac{C_{11}C_{33}C_{44}-C_{33}C_{14}^2-C_{44}C_{13}^2}{C_{33}C_{44}C_{11}^2-2C_{11}C_{33}C_{14}^2-C_{33}C_{44}C_{12}^2-2C_{12}C_{33}C_{14}^2-2C_{11}C_{44}C_{13}^2+2C_{12}C_{44}C_{13}^2+4C_{13}^2C_{14}^2} \quad (1)$$

$$S_{12}=\frac{C_{12}C_{33}C_{44}+C_{33}C_{14}^2-C_{44}C_{13}^2}{C_{33}C_{44}C_{11}^2-2C_{11}C_{33}C_{14}^2-C_{33}C_{44}C_{12}^2-2C_{12}C_{33}C_{14}^2-2C_{11}C_{44}C_{13}^2+2C_{12}C_{44}C_{13}^2+4C_{13}^2C_{14}^2} \quad (2)$$

$$S_{13}=-\frac{C_{13}}{C_{11}C_{33}+C_{12}C_{33}-2C_{13}^2} \quad (3)$$

$$S_{14}=-\frac{C_{14}}{C_{11}C_{44}-C_{12}C_{44}-2C_{14}^2} \quad (4)$$

$$S_{33}=\frac{C_{11}+C_{12}}{C_{11}C_{33}+C_{12}C_{33}-2C_{13}^2} \quad (5)$$

$$S_{44}=\frac{C_{11}-C_{12}}{C_{11}C_{44}-C_{12}C_{44}-2C_{14}^2} \quad (6)$$

$$S_{66}=2(S_{11}-S_{12}) \quad (7)$$

The compliance coefficient S_{ij} can be calculated as: S_{11}=0.00629, S_{33}=0.00590, S_{44}=0.02895, S_{12}=-0.00172, S_{13}=-0.00142, S_{14}=-0.00303. From the definition, we can obtain: E_x=E_y=158.583GPa, E_z=168.379GPa.

3.2.2 Reuss bound and Voigt bound

Reuss bound and Voigt bound of trigonal crystals are [14]:

$$G_V = \frac{(C_{11}+C_{22}+C_{33})-(C_{12}+C_{23}+C_{31})+3(C_{44}+C_{55}+C_{66})}{15} \quad (8)$$

$$G_R = \frac{15}{4(S_{11}+S_{22}+S_{33})-4(S_{12}+S_{23}+S_{31})+3(S_{44}+S_{55}+S_{66})} \quad (9)$$

$$B_V = \frac{C_{11}+C_{22}+C_{33}+2(C_{12}+C_{23}+C_{31})}{9} \quad (10)$$

$$B_R = \frac{1}{S_{11}+S_{22}+S_{33}+2(S_{12}+S_{23}+S_{31})} \quad (11)$$

Based on the Reuss bound and Voigt bound, elastic moduli can be obtained [9-10], which are as: G_v=55.99GPa, B_v=107.63GPa, G_r=48.18GPa, B_r=107.62GPa, B=107.63GPa, G=52.09GPa, E=134.56GPa, μ=0.292. Besides, values of the B (107.63GPa) and G (47.76GPa) are consistent with the values of 114.3GPa and 49.8GPa by the experimental measurement of Chen [2].

3.3 Elastic moduli under various pressures

3.3.1 Surface of elastic modulus

Surface of elastic modulus by DFT calculation of manganese carbonate is shown in Fig.4.

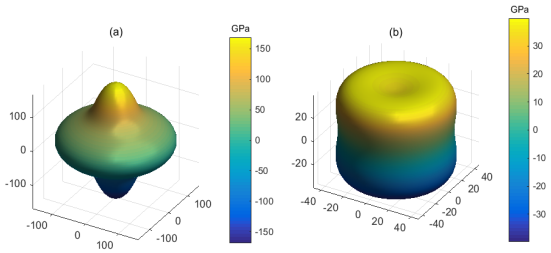

a)Young's modulus; b)Shear modulus;

Figure 4. Surface of elastic modulus by DFT calculation of manganese carbonate

From Fig.4, it can clearly be seen that Young's modulus and shear modulus are anisotropic, which is the same with the conclusion of fractional anisotropy. Elastic moduli of manganese carbonate based on C_{ij} can be calculated by Reuss-Voigt-Hill (RVH) estimation[9-10]. Young's modulus E of manganese carbonate is 134.56 GPa, which demonstrates manganese carbonate is a relatively stiffer material. Poisson ratio is 0.292.

3.3.2 Elastic moduli under various pressures

Young's modulus and shear modulus under different pressures is shown in Fig.5.

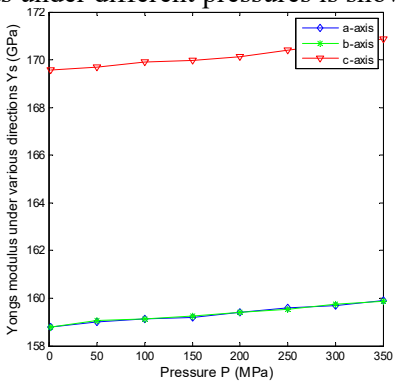

(a)Young's modulus;

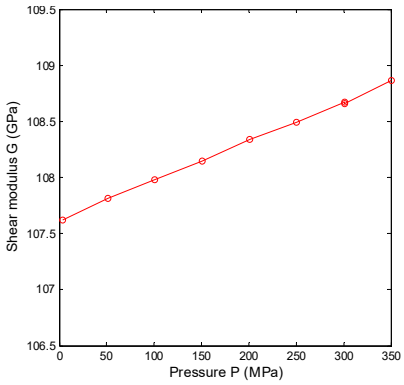

(b) Shear modulus

Figure 5. Curve of Young's modulus and shear modulus under different pressures

From Fig. 5(a), under 0-350 MPa, Young's modulus increases linearly in three directions, and in *c*-axis direction it increases significantly compared to the other two directions. This can be explained by the fact that the crystal structure alternates with the plane of the manganese ion and the CO_3 group in the *c*-axis direction. The shear modulus within the range of the pressure from 0 MPa to 350 MPa shows a linear change, rising from 107.682 GPa to 108.81 GPa, as in Fig. 5(b).

4. Conclusion

Based on MD method, the appropriate interatomic potential functions are used to describe the interaction between atoms in the process of energy minimization. The elastic constants C_{ij} of manganese carbonate crystal are calculated, and the C_{ij} variation under different pressures is discussed. Results are as:

(1) With the increase of the pressure, the lattice angles α, β, and γ change very little, while the lattice length (*a*, *b*, *c*) and the crystal volume *V* decrease continuously.

(2) With the increase of the pressure, rigid modulus and shear modulus increased significantly. Besides, the elastic constant C_{11} and C_{33} tend to increase while the other constants remain relatively stable.

(3) The molecular dynamics method is used to simulate the bulk modulus and shear modulus with the value of 107.63 GPa and 52.09 GPa, which is very close to the experimental measurement and theoretical values. Thus, the validity of the simulation method and the reliability of the initial parameters are verified.

References

[1] Jia Fu, Fabrice Bernard, Siham Kamali-Bernard, Molecular Simulation, **44**(4), 285-299 (2018).
[2] Chen C.C., Lin C.C., Liu L.G., Sinogeikin S.V, and Bass J.D., AM, **86**, 1525–1529 (2001).
[3] Wang Q., Grau-Crespo R., and de Leeuw N.H, J. Phys. Chem. **B115**, 13854–13861 (2011).
[4] Zhang J. and Reeder R.J., American Mineralogist, **84**, 861–870(1999).
[5] Po-Fei Chen, Ling-Yun Chiao, et al., Physics of the Earth and Planetary Interiors, **155**, 73–86 (2006).
[6] Jia Fu, K.-B. Siham, B. Fabrice, Marilyne Cornen, Compos Part B-Eng, **150**, 1-15 (2018).
[7] Jia Fu, B. Fabrice, K.-B. Siham, J Phys Chem Solids,**101**,74-89 (2017).
[8] Jia Fu, B. Fabrice, K.-B. Siham, J Nano Res. **33**, 92-105 (2015).
[9] Jia Fu, Weihui Lin, Zhongren Chen. IJAMP,**1**(1), 62-69 (2016).
[10] Jia Fu,Weihui Lin, *AER,* **120**, 390-395 (2017).
[11] Austen KF., Wright K., Slater B., and Gale JD, PCCP, **7**, 4150–4156 (2005).
[12] Maslen E. N. Streltsov V. A. And Streltsova N. R., Acta Cryst, **B51**, 929-939 (1995).
[13] J. F. Nye, Physical Properties of Crystals, *Oxford University Press*, Oxford, 1985.
[14] W. Pabst, G. Tichá, E. Gregorová , Ceramics Silikaty, **48**(2), 41-48 (2004).